Received: 4 September 2019 | Revised: 11 August 2020 | Accepted: 31 August 2020

DOI: 10.1096/fj.201902202R

RESEARCH ARTICLE

THE FASEB JOURNAL

A dual role for *Tbx1* in cardiac lymphangiogenesis through genetic interaction with *Vegfr3*

Stefania Martucciello[1,2] | Maria Giuseppina Turturo[3] | Marchesa Bilio[3] | Sara Cioffi[3] | Li Chen[4] | Antonio Baldini[3,5] | Elizabeth Illingworth[2]

[1]IRCCS Neuromed, Pozzilli, Italy

[2]Department of Chemistry and Biology, University of Salerno, Fisciano, Italy

[3]Institute of Genetics and Biophysics "ABT", CNR, Naples, Italy

[4]Department of Biology and Biochemistry, University of Houston, Houston, TX, USA

[5]Department of Molecular Medicine and Medical Biotechnology, University of Naples Federico II, Naples, Italy

Correspondence
Elizabeth Illingworth, Department of Chemistry and Biology, University of Salerno, Via Giovanni Paolo II, 132, Fisciano 84084, Italy.
Email:eillingworth@unisa.it

Funding information
Fondation Leducq, Grant/Award Number: 15CVD01; Ministero della Salute (Ministry of Health, Italy), Grant/Award Number: RF-2011-02347197 and 20179J2P9J; Fondation Jérôme Lejeune (Jerome Lejeune Foundation), Grant/Award Number: 1685

Abstract

The transcription factor *TBX1* is the major gene implicated in 22q11.2 deletion syndrome (22q11.2DS). The complex clinical phenotype includes vascular anomalies and a recent report presented new cases of primary lymphedema in 22q11.2DS patients. We have previously shown that TBX1 is required for systemic lymphatic vessel development in prenatal mice and it is critical for their survival postnatally. Using loss-of-function genetics and transgenesis in the mouse, we show here a strong genetic interaction between *Tbx1* and *Vegfr3* in cardiac lymphangiogenesis. Intriguingly, we found that different aspects of the cardiac lymphatic phenotype in *Tbx1-Vegfr3* compound heterozygotes were regulated independently by the two genes, with *Tbx1* primarily regulating vessel numbers and *Vegfr3* vessel morphology. Consistent with this observation, $Tbx1^{Cre}$-activated expression of a *Vegfr3* transgene rescued partially the cardiac lymphatic abnormalities in compound heterozygotes. Through time-controlled genetic experiments, we show that *Tbx1* is activated and required in cardiac lymphatic endothelial cell (LEC) progenitors between E10.5 and E11.5. Furthermore, we found that it is also required later in development for the growth of the cardiac lymphatics. Finally, our study revealed a differential sensitivity between ventral and dorsal cardiac lymphatics to the effects of altered *Tbx1* and *Vegfr3* gene dosage, and we show that this likely results from an earlier requirement for *Tbx1* in ventral cardiac LEC progenitors.

KEYWORDS

cardiac, genetic interaction, lymphatic vessel, mouse model, *Tbx1*, *Vegfr3*

Abbreviations: CHD, congenital heart disease; DAB, 3,3′-diaminobenzidine; DAPI, 4′,6-diamidino-2-phenylindole; EC, endothelial cell; EGFP, enhanced green fluorescent protein; ER, estrogen receptor; ES, embryonic stem; HRP, horseradish peroxidase; IRES, internal ribosome entry site; KD, knockdown; LV, left ventricle, RV, right ventricle; LYVE1, lymphatic endothelial hyaluronan receptor 1; MAPK, mitogen-activated protein kinase; MCS, multiple cloning site; OFT, outflow tract; PBS, phosphate-buffered saline; pERK, phosphorylated-extracellular receptor kinase; Prox1, Prospero homeobox protein 1; PVDF, polyvinylidene difluoride; R26R, Rosa26 reporter; SDS-PAGE, sodium dodecyl sulfate- polyacrylamide gel electrophoresis; SHF, secondary heart field; SV, sinus venosus; TBX1, Tbox1; Tg, transgenic; TM, tamoxifen; TOF, tetralogy of Fallot; Vegfr3, vascular endothelial growth factor receptor 3; WT, wild-type; 22q11.2DS, 22q11.2 deletion syndrome.

Stefania Martucciello and Maria Giuseppina Turturo contributed equally to this work.

1 | INTRODUCTION

In the mammalian heart, the primary role of the cardiac lymphatic vasculature is to maintain fluid homeostasis and transport immune cells. In the mouse, the cardiac lymphatic network develops from lymphatic endothelial cells (LECs) that migrate into the heart around embryonic day (E) 12.5. As embryonic development progresses, an extensive network of subepicardial lymphatic vessels forms, extending over the heart from base to apex and covering mainly the left ventricle, both ventrally and dorsally, while fewer lymphatic vessels extend over the right ventricle[1-3] Development of the cardiac lymphatic vessel network is complete by postnatal day (P) 15.

Tbx1 is a major developmental gene for which a critical role in lymphangiogenesis has been demonstrated in the mouse.[4] In the absence of *Tbx1*, most lymphatic vessels are lost around E16.5. We have shown that TBX1 regulates *Vegfr3* expression in ECs by binding to an intragenic enhancer element in the endogenous *Vegfr3* gene. In *Tbx1* germline mutants, and in EC-specific conditional *Tbx1* mutants, *Vegfr3* expression in LECs is lost between E15.5 and E16.5, which led us to hypothesize that lymphatic vessels in *Tbx1* mutants are not maintained because of reduced *Vegfr3* expression in LECs.[4]

In this study, we tested this hypothesis by manipulating the dosage of both genes in ECs in vivo. We focused our attention on cardiac lymphangiogenesis because the cardiac lymphatic phenotype is severe in *Tbx1* mutant mice [4] and because cardiac neo-lymphangiogenesis has been implicated in the response to ischemia[2,5,6] through the upregulation of developmental lymphatic genes, including *Vegfr3*. Furthermore, post-infarct cardiac function improved after treatment with recombinant VEGF-C,[2] suggesting that signaling through the Vegf-C-Vegfr3 pathway is important for responding to pathological conditions of the heart.

We found a strong interaction between *Tbx1* and *Vegfr3* in cardiac lymphangiogenesis. Increasing endothelial expression of *Vegfr3* from a transgene was sufficient to rescue in part the cardiac lymphatic phenotype in compound heterozygotes, indicating that VEGFR3 is a major effector of TBX1 function in lymphatic vessels. However, it did not improve cardiac lymphatic development in *Tbx1* homozygous mutants, which lack lymphatic vessels in most tissues, including the heart. We then determined the critical time requirement for *Tbx1* in cardiac lymphangiogenesis through time-controlled gene inactivation. Results showed that *Tbx1* is required prior to the onset of cardiac lymphangiogenesis, suggesting that it might play a critical role in cardiac lymphatic endothelial progenitors. We then used time-controlled *Tbx1*-lineage tracing to determine when *Tbx1*-expressing cells, or their descendants, contribute to cardiac lymphatics. Interestingly, our results indicate a bi-phasic requirement for *Tbx1* in cardiac lymphangiogenesis.

2 | MATERIAL AND METHODS

2.1 | Mouse lines and tissues

The following mouse lines were used: $Tbx1^{lacZ/+}$,[7] $Tbx1^{flox/+}$,[8] $Tbx1^{Cre/+}$,[9] $Tbx1^{mcm/+}$,[10] Tie2Cre,[11] $Vegfr3^{flox/+}$,[12] R26R,[13] $Rosa^{mTmG}$,[14] CAGG-CreER,[15] *Mef2C*-AHF-Cre mice.[16] To generate $Vegfr3^{+/-}$ mice, we crossed female *Mef2C*-AHF-Cre mice with male $Vegfr3^{flox/+}$ mice. The progeny from this cross with the genotype $Vegfr3^{+/-}$ was crossed with wild-type mice (C57BL/6) in order to recover F2 $Vegfr3^{+/-}$ mice. The latter cross was performed in order to avoid mosaicism. Genotyping of mice was performed according to the original reports. Activation of CAGG-CreER was performed with a single intraperitoneal injection of Tamoxifen (Sigma) at 75 mg/kg body weight at one of various time points between gestation days 10.5 and 16.5.

2.2 | Salmon-gal staining, immunohistochemistry, and immunofluorescence

Beta-Gal activity was revealed by salmon-gal staining. Embryonic hearts at E14.5, E15.5, and E18.5 were isolated and fixed for 30 minutes in glutaraldehyde (0.2%), paraformaldehyde (2%), EGTA (5 mM), magnesium chloride (2 mM), and phosphate buffer at pH 7.3 (0.1 M), then, washed three times (20 min per wash) in a solution containing sodium deoxycholate (0.1%), NP40 (0.2%), magnesium chloride (2 mM), and phosphate buffer pH 7.3 (0.1M). Hearts were stained in a solution containing Salmon-Gal (Thermo Fisher Scientific) at 1 mg/mL and NBT (Roche) at 0.4 mM in washing solution in the dark at 37°C with gentle rotation until the desired staining was achieved. Immunostaining was performed using the following primary antibodies: rat anti-VEGFR3 (eBioscience), rabbit anti-LYVE1 (Abcam), rabbit anti-GFP (Invitrogen), anti-ENDOMUCIN, anti-CD31, mouse anti-pERK (Cell Signaling), diluted 1:400, and secondary antibodies: HRP-conjugated goat anti-rat IgG (Kirkegaard & Perry Laboratories), HRP-conjugated anti-rabbit IgG (GE Healthcare), diluted 1:200. Fluorescent antibodies were visualized using Vectashield imaging medium (Vector Laboratories). Nonfluorescent antibodies were visualized using DAB (Vector Laboratories). Whole-mount specimens were photographed using a dissecting microscope (Stemi 2000; Carl Zeiss, Inc) equipped with a camera (Axiocam; Carl Zeiss, Inc) and the manufacturer's acquisition software. Images were acquired at 28x magnification.

2.3 | Quantitative analysis of lymphatic vessel anomalies

We analyzed a minimum of five and a maximum of eight embryos per genotype in all experiments. Three-dimensional images were digitally reconstructed from *z* stacks. For each image, we manually counted all the lymphatic vessels on the dorsal and ventral surfaces of the heart, and we measured the length and area of each vessel. We then calculated the ratio length/area to determine the width of each single vessel. Quantitative analysis was performed using the ImageJ software, (www.uhnresearch.ca/facilities/wcif/imagej).

2.4 | Statistical analysis of lymphatic vessels

We used the nonparametric Kruskal-Wallis test for the analysis of lymphatic vessels in all experiments with a single exception, namely *Vegfr3*$^{+/-}$ vs WT embryos, for which the Mann-Whitney *U* test was used. We first calculated the mean number of vascular features (number, length, area/length vessels) for each embryo. We then calculated the mean value for the group (same genotype). The latter value was used for the statistical analysis. *P* values of $<.05$ were considered as statistically significant. Error bars represent standard deviation.

2.5 | Generation of transgenic mouse embryonic stem cells

The starting vector was the pCIG2 plasmid[17] without the nuclear localization sequence of EGFP-CDS that consists of a CMV-IE enhancer, chicken beta-actin promoter, MCS, IRES-GFP, and rabbit beta-globin polyA. A loxP-flanked neomycin resistance cassette was cloned downstream of the beta-actin promoter followed by a full-length mouse *Vegfr3* cDNA (GeneCopoeia), (Supporting Figure S4A) The linearized Vegfr3 transgenic construct, named TgVegfr3, was electroporated into feeder-free E14Tg2A.4 mouse ES cells using the ECM 630 Electro Cell Manipulator System (BTX). Twenty-four hours post-electroporation, the cells were selected in G418 at a final concentration of 250 μg/mL. ES cell clones were picked 12 days after plating.

2.6 | Identification of correctly targeted ES cell clones by southern blotting

Two probes were generated for southern blotting experiments. To identify clones with a single insertion of the transgene, a region of the neomycin resistance cassette was amplified by PCR using the primers: pF 5′ GCACAACAGACAATCGGCTG 3′, pR 5′GATACTTTCTCGGCAGGAGC 3′. The first probe, which was designed upstream the first BamHI cutting site in the linearized TgVegfr3 construct, localized within the neomycin-resistance cassette. The first BamHI cutting site upstream of the region amplified localized to genomic DNA, and thus, its position depended upon the insertion site of the electroporated TgVegfr3 construct. Thus, the size of the fragment recognized by this probe varied from clone to clone, and within in the same clone, from insertion to insertion, in the case of multiple integrations of the transgene (Supporting Figure S4B). ES cell clones containing a single copy of TgVegfr3 were analyzed by PCR to confirm that the entire *Vegfr3* cDNA was present, using the primers: pF 5′CGACGAATTCGGTACCATGCAG 3′, pR 5′GCACGGACTGGCCTTCTAAG 3′. These primers amplified a region extending from 16 bp upstream of the ATG to 20 bp downstream of the BamHI site. A 1741 bp fragment was expected. The second probe distinguished the transgene from the endogenous *Vegfr3* gene. It was generated by PCR amplifying a segment of exon 13 of the *Vegfr3* cDNA, using the following primers: pF 5′CTTAGAAGGCCAGTCCGTGC 3′, pR 5′CCTGCACGGACAGGTACTTC 3′. BamHI digestion of genomic DNA from ES clones generated a 2.5Kb fragment in the presence of the transgene and a 2.8 Kb fragment in the endogenous *Vegfr3* gene (Supporting Figure S4C).

2.7 | Generation of transgenic mice

Two correctly targeted ES cell clones were selected for microinjection into mouse blastocysts. Four males chimeras were obtained. These males were bred with black C57BL/6 female mice and three germ line transmissions were obtained. These founders were crossed into the C57BL/6 strain. Mice were genotyped by PCR using DNA extracted from tail biopsies, using following primer pairs: F-5′-ATCGACCTGGCAGACTCCAA-3′; R-5′-GAAAACTGCGATGACGCCAGT-3′. PCR products were separated on 2% of agarose gels.

2.8 | Characterization and functional testing of the TgVegfr3 transgene

We characterized the transgenic VEGFR3 protein in cells and in mice. We first tested whether Cre activation of the transgene led to the production of a full-length VEGFR3 protein. For this, we co-transfected C2C12 cells, which do not express *Vegfr3*, with the transgene, and a Cre-expressing vector. Western blotting with anti-VEGFR3 antibody performed 24 hours after transfection revealed the presence of a protein of the expected length of 195 KDa (Supporting Figure S4D). Furthermore, anti-VEGFR3 immunocytofluorescence performed on the same cells indicated that the transgenic protein localized to the cell membrane (Supporting Figure S4E). In

order to confirm that the transgene localized correctly and functioned in vivo, we crossed TgVegfr3 mice with *Tbx1*$^{Cre/+}$ mice and analyzed expression of VEGFR3 (Supporting Figure S4F) and phosphorylated ERK (pERK, Supporting Figure S4G) in embryos at E15.5. We observed ectopic expression of the transgenic VEGFR3 protein in the tongue (Supporting Figure S4F, a′), heart (Supporting Figure S4F, b′,c′), and mandibular (masseter) muscle (Supporting Figure S4G, a′) in E15.5 *Tbx1*$^{Cre/+}$; TgVegfr3 embryos but not in *Tbx1*$^{Cre/+}$ (control) embryos (Supporting Figure S4F, a-c, Figure S4G, a). Similarly, pERK was expressed in the masseter muscle of *Tbx1*$^{Cre/+}$; TgVegfr3 embryos (Supporting Figure S4G, b′) but not in *Tbx1*$^{Cre/+}$ (control) embryos (Supporting Figure S4G, b). These results indicate that *Tbx1*^{Cre} activates expression of transgenic *Vegfr3* in the endogenous *Tbx1* expression domains and that the transgenic protein is able to activate the MAPK/ERK pathway, a known signaling pathway downstream of VEGF-C/VEGFR3 that promotes cell proliferation.

2.9 | Western blot analysis

Transfected C2C12 cells were collected 24 hours after transfection, washed with PBS and lysed in lysis buffer (Tris-HCl 20 mM pH7.4, NaCl 100 mM, 10 mM MgCl2, NP-40 1X, Glycerol 10%, protease inhibitors). Denatured proteins were separated by SDS-PAGE, transferred to Immuno-Blot PVDF Membrane (BioRad) for protein blotting, Membranes were blocked for 1 hour at RT in TBST (150 mM NaCl, 10 mM Tris-HCl, pH 7.4, and 0.05% Tween) and powdered milk. The membranes were incubated overnight at 4°C in primary antibodies diluted in TBST-5% of milk, then, for 1 hour at RT with horseradish peroxidase-conjugated secondary antibodies (diluted in TBST-5% milk). Protein binding was detected by ECS (Amersham) using Hyperfilm (Amersham). The molecular masses of proteins were estimated relative to the electrophoretic mobility of the co-transferred, pre-stained protein marker All Precision Blue (BioRad). The primary antibodies used were rat anti-VEGFR3 (eBioscience), rabbit anti-GFP (Sigma-Aldrich).

2.10 | Immunofluorescence on C2C12 cells

C2C12 cells were plated into 6-well plates on coverslips. The next day, cells were co-transfected with the TgVegfr3 construct and Cre recombinase vector. Immunocytofluorescence was performed 24 hours after transfection. Cells were washed and fixed with 3% of paraformaldehyde/PBS for 20 minutes at RT, permeabilized with 0.1% of Triton X-100/PBS for 25 minutes, and blocked with 1% of BSA/PBS for 45 minutes. Cells were incubated with anti-VEGFR3 antibody (eBioscience) diluted 1:100 in 0.1% of BSA/PBS for 3 hours, washed three times with PBS, incubated for 1 hour with secondary antibody Alexa Fluor anti-rat 494 nm (Invitrogen) 1:200 in PBS. The fluorescent antibody was visualized using imaging medium (Vectashield with DAPI, Vector Laboratories). For visualization, the coverslip was positioned on a slide and images were acquired using confocal microscopy.

2.11 | Cell culture and transfections

Human microvascular lymphatic endothelial cells, HMLECs (Lonza) were grown in EGM-2 Bullet Kit (Lonza) to 80% confluence and transfected with 40 nM siRNA and Lipofectamine 2000 (Invitrogen). RNA interference was performed using a commercial siRNAs against *TBX1* and *VEGFR3* (ON-TARGETplus SMARTpool, Thermo Fisher Scientific) and a control non-targeting (NT) siRNA (Thermo Fisher Scientific). Cells were collected 24 hours after transfection. For experiments involving knockdown of both genes, siRNA-transfected cells were re-transfected with the second siRNA after 24 hours, using the same experimental conditions. Cells were collected 24 hours after the second transfection.

2.12 | RNA transfection, cDNA synthesis, and quantitative RT-PCR

cDNA was synthesized from 1 µg of total RNA isolated from HMLECs using the QuantiTect Reverse Transcription Kit (Qiagen) according to the manufacturers instructions. Quantitative real-time PCR was performed using Universal SYBR Green Supermix (Bio-Rad). Relative quantification of gene expression was performed using the comparative cycle threshold method (ΔCT) with *GAPDH* as the reference gene.

2.13 | Human primer sequences used for qReal-Time PCR

h TBX1_F: 5′-GGACGACAACGGCCACAT-3′
h TBX1_R: 5′-CGGCATATTTCTCGCTATCT TTG-3′
h DLL4_F: 5′-CATTGGACTATAATCTGGCC CC-3′
h DLL4_R: 5′-ATCCGACACTCTGGCTTTT C-3′
h VEGFR3_F: 5′-AACGACACAGGCAGCTAC GTC-3′
h VEGFR3_R: 5′-GATGAATGGCTGCTCAA AGTCTC-3′
h UNC5B_F: 5′-AAACTCTAAGCGACCCC AAC-3′

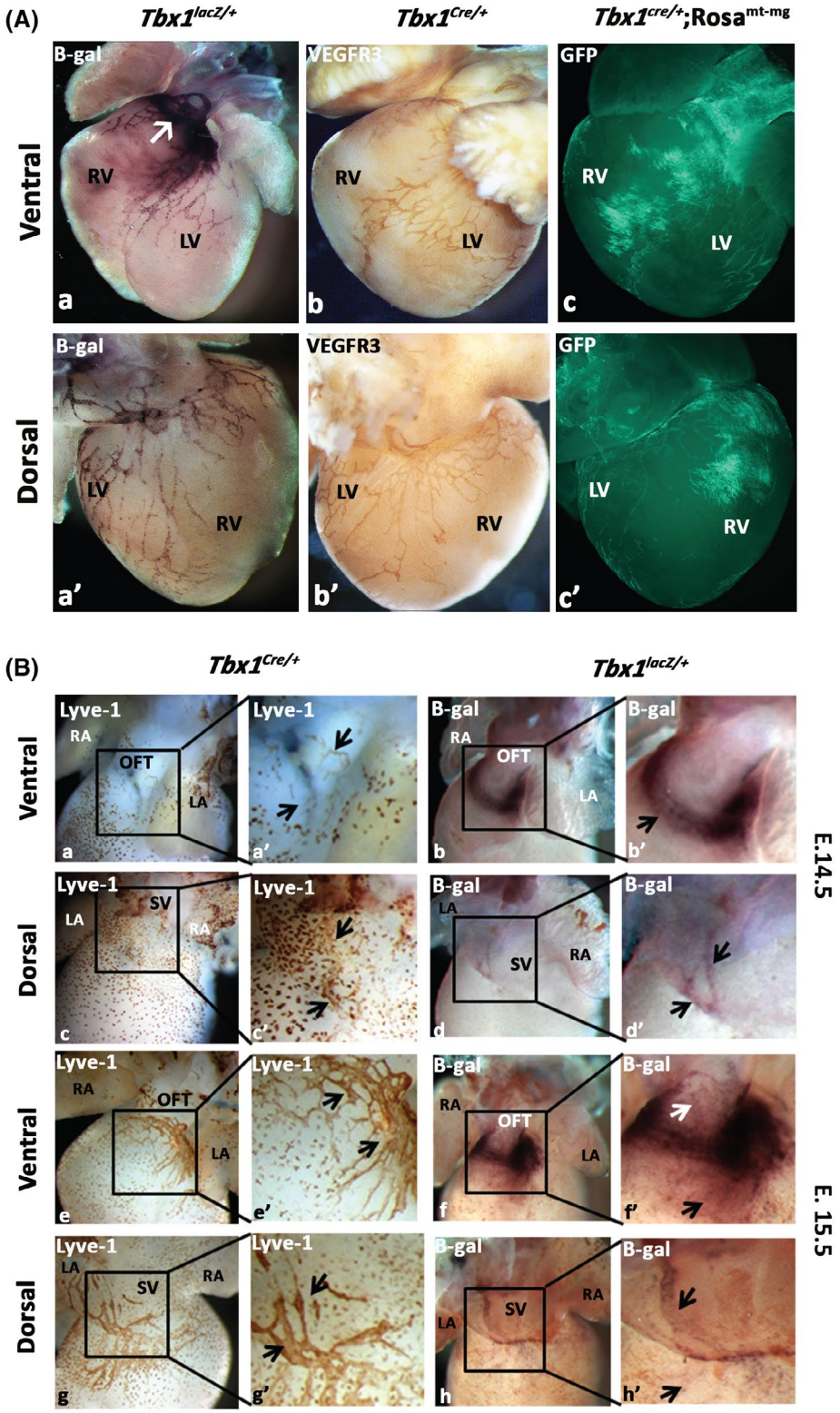

FIGURE 1 *Tbx1* and *Vegfr3* are co-expressed in cardiac lymphatic vessels. A, beta-gal staining of E18.5 $Tbx1^{lacZ/+}$ hearts shows that *Tbx1* is expressed in the conotruncus (arrow in a) and in cardiac lymphatic vessels (a-a′), identified by anti-VEGFR3 immunostaining (b-b′). Fate mapping of *Tbx1*-expressing cells and their descendents in $Tbx1^{cre/+}$; $Rosa^{mT\text{-}mG}$ hearts (c-c′) reveals a contribution to cardiac lymphatic vessels and to the right ventricular myocardium. B, VEGFR3 immunostaining (left) of E.14.5 (a-d) and E.15.5 (e-h) $Tbx1^{Cre/+}$ hearts reveals cardiac lymphatic vessels (arrows in a′, c′, e′, g′). Beta-gal staining (right) of E.14.5 (b, b′, d, d′) and E.15.5 (f, f′, h, h′) $Tbx1^{lacZ/+}$ hearts shows that *Tbx1* is expressed in lymphatic vessels at the base of the outflow tract ventrally (arrows in b′, f′) and in the sinus venosus dorsally (arrows in d′, h′). Scale bar 100 μm

h UNC5B_R: 5′-TCGAAGTCACGGCAGTTG-3′
h HEY1_F: 5′-TGGTACCCAGTGCTTTTGAG-3′
hHEY1_R:5′-CTCCGATAGTCCATAGCAAGG-3′
h NRARP_F: 5′-CAGCGCATCTTCCAGGAG-3′
h NRARP_R: 5-TCGCAGTTGGTCATGTTCTG-3
GAPDH_F: 5′-TGCACCACCAACTGCTTAGC-3′
GAPDH_R: 5′-TCTTCTGGGTGGCAGTGATG-3′
h VEGFR2_F: 5′-ATAGAAGGTGCCCAGGAAAAG-3′
h VEGFR2_R: 5′-GTCTTCAGTTCCCCTCCATTG-3′
hNOTCH1_F:5′-TGCCTGGACAAGATCAATGAG-3′
hNOTCH1_R:5′-CAGGTGTAAGTGTTGGGTCC-3′

2.14 | Migration assay

Transwell filters coated with collagen in serum-free EBM-2 Basal Media containing 0.1% of BSA, with a PET membrane with 8 μm pores (BD Biosciences), were rehydrated for 2 hours at 37°C without supplements. Transfected cells were washed once in PBS, and 20^5 cells were seeded into the upper chamber of the Transwells in serum-free media containing 0.1% of BSA. Media containing VEGF-C (9199-vc R&D) [50 ng/mL] or 0.1% of BSA was added to the lower chamber as a chemoattractant. Control wells without VEGF-C were included to assess random migration. Cells were allowed to migrate for 16 hours at 37°C, in 5% of CO_2. The cells adhering to the underside of the membrane were fixed with 4% of paraformaldehyde in PBS for 10 minutes, and then, stained with 0.5% of Crystal Violet in 20% of methanol for 20 minutes. The cells on the lower side of the filter were allowed to dry before counting. Eight separate bright field images were randomly acquired of each filter using an Olympus CKX41 Image Analyzer. The cells in each image were counted and analyzed in comparison to control-transfected cells.

2.15 | Statistical analysis of cell-based studies

Statistical significance was determined by the two-tailed paired Student's *t* test, except for the cell migration assay, which was analyzed by a chi-square test. *P* values of <.05 were considered as statistically significant. Error bars represent standard deviation.

3 | RESULTS

3.1 | *Tbx1* and *Vegfr3* are co-expressed in cardiac lymphatics

We have previously shown that TBX1 regulates *Vegfr3* expression in ECs by binding to an intragenic enhancer element in the endogenous *Vegfr3* gene.[4] *Tbx1* expression in the heart has been noted,[4,18] but it has not been reported in detail. We visualized *Tbx1* expression using a *lacZ* reporter allele[7] and monitored its expression by beta-galactosidase (beta-gal) activity in $Tbx1^{lacz/+}$ (heterozygous) hearts at E18.5 (Figure 1). This revealed beta-gal + vessels on the ventral and dorsal surfaces of the heart that resembled lymphatic vessels (Figure 1A, a,a′) and beta-gal + cells in the sub-pulmonary myocardium (arrow in Figure 1A, a), as previously reported.[10,18] To verify the lymphatic identity of the beta-gal + vessels, we immunostained hearts of *Tbx1* heterozygous embryos ($Tbx1^{Cre/+}$)[9] at E18.5 with anti-VEGFR3 antibody, which specifically labels lymphatic ECs at this developmental stage.[19] Results showed that *Tbx1* (Figure 1A, a,a′) and *VEGFR3* (Figure 1A, b,b′) had near identical expression, suggesting that they are co-expressed in cardiac lymphatic vessels at this stage of development.

In the mouse, the cardiac lymphatic vasculature begins to form around E12.5 at the sinus venosus on the dorsal surface of the heart and ventrally at the outflow tract (OFT).[1-3,20] From E14.5, a network of subepicardial lymphatic vessels spreads over the ventricles in a basal to apical direction, reaching maturity at postnatal day (P) 15.[1,2] We asked whether *Tbx1* is expressed in early cardiac lymphatics. To address this question, we performed beta-gal staining and LYVE1 immunostaining on $Tbx1^{lacz/+}$ hearts at E14.5 and E15.5. LYVE1 is expressed by lymphatic ECs, but not by venous or arterial ECs in most organs, and also in tissue-resident macrophages (punctate signal in Figure 1B, left panel). Results showed that at E14.5 (Figure 1B, a-d) and E15.5 (Figure 1B, e-h), on the dorsal surface of the heart, LYVE1 + lymphatics at the sinus venosus (Figure 1B, c,c′,g,g′) expressed *Tbx1* (beta-gal+) (arrows in d′ and h′). The similar expression of the two markers was less visible on the ventral surface of E14.5 hearts, because *Tbx1* is highly expressed in the sub-pulmonary myocardium (arrow in b′), where the first ventral lymphatic vessels form (arrows in a′). However, at E15.5, a small network of LYVE1 + vessels on the ventral surface of the outflow tract, and on the heart (black arrows in e′) was beta-gal+ (white and black arrows respectively in f′).

As the $Tbx1^{lacZ}$ reporter allele is rather weak, and cannot be used in conjunction with fluorescent antibodies for co-localization studies, we verified the expression of *Tbx1*

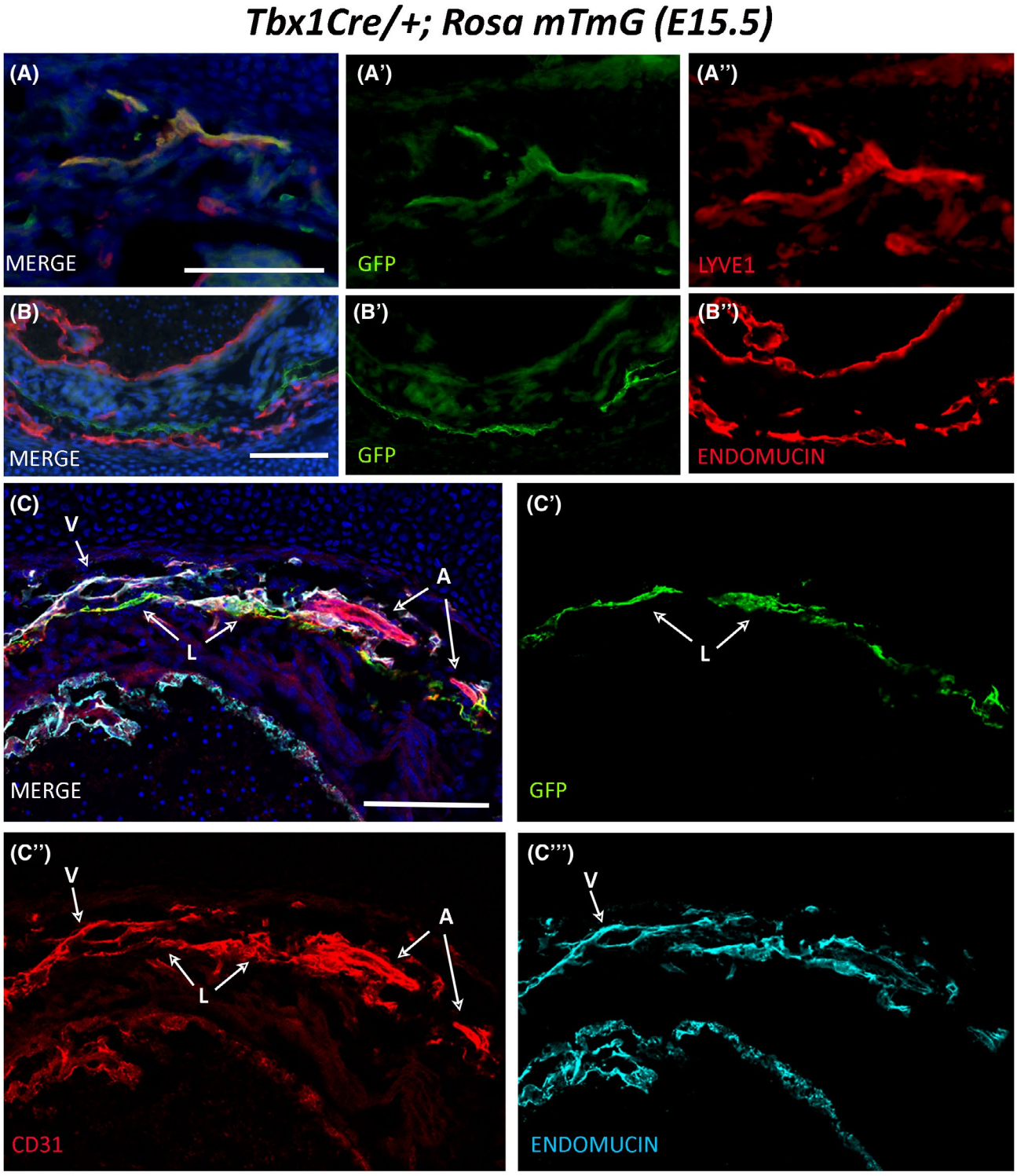

FIGURE 2 TBX1 is expressed in cardiac lymphatic vessels but not in cardiac arteries and veins. A, Co-immunostaining with anti-GFP (a′) and anti-LYVE1 (a′′) antibodies reveals the co-localization of the two proteins in cardiac lymphatic vessels in $Tbx1^{cre/+}$; $Rosa^{mT\text{-}mG}$ embryos at E15.5 (a). B, The lack of co-localization of the GFP (b′) and Endomucin (b′′) proteins demonstrates that TBX1 is not expressed in cardiac veins. C, Simultaneous immunostaining with anti-GFP, anti-CD31, and anti-Endomucin demonstrates that TBX1 is not expressed in coronary arteries (CD31+; Endomucin-). A, artery, V, vein, L, lymphatic vessel. Scale bars 100 μm

in cardiac lymphatics by using an alternative *Tbx1* allele, $Tbx1^{Cre/+9}$ For this, we crossed $Tbx1^{Cre/+}$ mice with $Rosa^{mT\text{-}mG}$ mice[14] and analyzed the hearts of $Tbx1^{Cre/+}$; $Rosa^{mT\text{-}mG}$ embryos at E15.5, where *Tbx1*-expressing cells and their descendants were irreversibly labeled by $Tbx1^{Cre}$-activated expression of GFP. We then stained serial transverse sections of

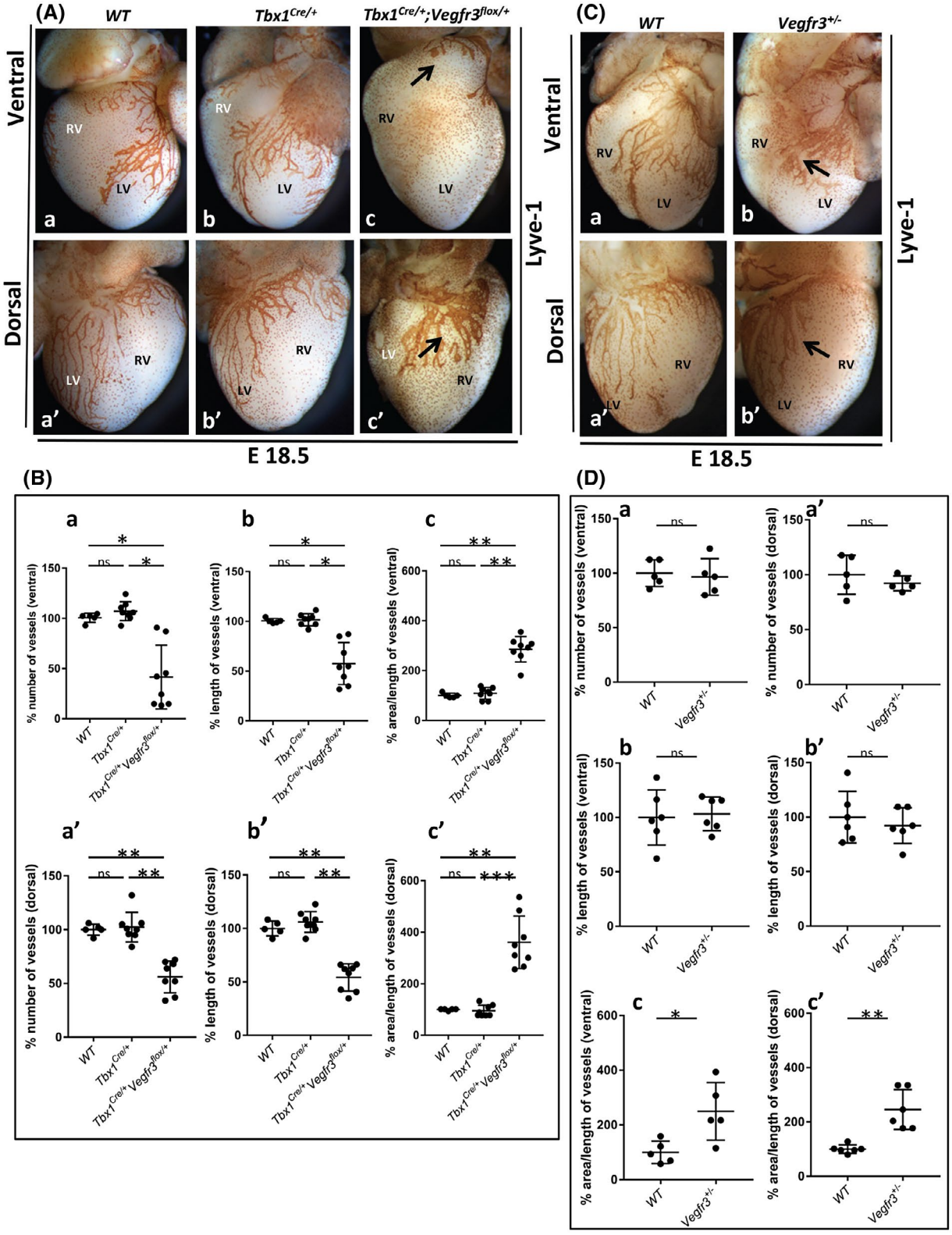

FIGURE 3 Genetic interaction between *Tbx1* and *Vegfr3* in cardiac lymphatic development. A and C, Anti-LYVE1 immunostaining identifies subepicardial lymphatic vessels in representative hearts of E18.5 embryos of the genotypes shown (punctate signal derives from LYVE1 + macrophages). A, Arrows in c, c′ indicate abnormal cardiac lymphatic vessels in compound heterozygous embryos. B, Quantitative analysis revealed a reduced number (a-a′) reduced length (b-b′) and increased width (c-c′) of ventral and dorsal cardiac lymphatic vessels in E18.5 $Tbx1^{Cre/+}$; $Vegfr3^{flox/+}$ embryos compared to *WT* (a-a′) and $Tbx1^{Cre/+}$ (control) embryos (b-b′). C, *Vegfr3 haploinsufficiency in cardiac lymphatic development*. LYVE1 immunostaining reveals mild hypertrophy of cardiac lymphatic vessels in E18.5 $Vegfr3^{+/-}$ embryos (b-b′). D, Quantitative analysis (D) shows that number (a-a′) and length (b-b′) of cardiac lymphatic vessels were normal, but they were moderately dilated (c-c′). LV, left ventricle, RV, right ventricle. $^{*}P < 0.05$, $^{**}P \leq .01$, $^{***}P \leq .001$. Error bars represent standard deviation

these hearts with anti-LYVE1 antibody. Results revealed the co-localization of the GFP and LYVE1 proteins in cardiac lymphatics (Figure 2A,A′′). Furthermore, the lack of GFP+; VEGFR3-negative cells suggests that in the mouse heart vessels, *Tbx1*-expressing cells and their progeny contribute exclusively to lymphatic vessels and not to veins or arteries. We tested this directly by co-immunostaining serial sections with anti-GFP and vessel-specific antibodies, namely, anti-ENDOMUCIN (labels veins), anti-CD31 (labels all vessels). Together, the results obtained from these experiments confirmed that *Tbx1* expression (GFP+) is activated in cardiac lymphatics (LYVE1+; CD31+, Figure 2A,A′′) but not in cardiac veins (ENDOMUCIN+; CD31+, Figure 2B,B′′) or arteries (CD31+; ENDOMUCIN-, Figure 2C). The lack of *Tbx1* expression in the coronary arteries has been reported.[18] *Tbx1*-expressing cells however, do contribute to endothelium of the cardiac outflow tract and to the fourth pharyngeal arch arteries.[10]

3.2 | *Tbx1* and *Vegfr3* interact genetically in cardiac lymphatic development

As *Tbx1* and *VEGFR3* were co-expressed in cardiac lymphatics, and we have previously shown that TBX1 regulates *Vegfr3*,[4] we next tested whether they interact genetically to regulate cardiac lymphangiogenesis. For this, we crossed $Tbx1^{Cre/+}$ with $Vegfr3^{flox/+}$ mice[12] and analyzed cardiac lymphatics in E18.5 $Tbx1^{Cre/+}$; $Vegfr3^{flox/+}$ embryos by whole-mount immunostaining with anti-LYVE1 antibody. We also generated $Vegfr3^{+/-}$ (germline heterozygous) mice by crossing $Vegfr3^{flox/+}$ mice with germline Cre-expressing mice.[16,21] We first analyzed the cardiac lymphatics in $Tbx1^{Cre/+}$ and $Vegfr3^{+/-}$ embryos compared to wild-type littermates. We quantified the number, length and width (ratio length/area) of lymphatic vessels in at least five E18.5 embryos per genotype, using the ImageJ software. In $Tbx1^{Cre/+}$ embryos, we found no differences in the number, length or width of cardiac lymphatics on either the ventral or dorsal surfaces of the heart (Figure 3A, b,b′ and Figure 3B, a,a′,b,b′,c,c′) compared to WT controls (Figure 3A, a,a′, Supporting Figure S6, Table 1). In $Vegfr3^{+/-}$ embryos, the number and length of cardiac lymphatics were normal (Table 1), but both ventral and dorsal lymphatic vessels were moderately dilated (Figure 3C, b,b′, Figure 3D, c,c′). As far as we are aware, this is the first demonstration that *Vegfr3* is haploinsufficient in murine cardiac lymphatic development. We next analyzed compound heterozygous embryos ($Tbx1^{Cre/+}$; $Vegfr3^{flox/+}$), and found that the cardiac lymphatic network was strongly reduced (Figure 3A, c,c′) compared to controls ($Tbx1^{Cre/+}$, $Vegfr3^{+/-}$, WT, Table 1), especially on the ventral surface of the heart where, in most embryos, only a few lymphatic vessels were present around the base of the pulmonary trunk and in the sub-pulmonary myocardium (arrow in Figure 3A, c′). Quantitative analysis confirmed the reduction in the number (Figure 3B, a,a′), length (Figure 3B, b,b′) and width (Figure 3B, c,c′) of ventral and dorsal cardiac lymphatics in compound heterozygous embryos. Together, these results demonstrate a strong genetic interaction between *Tbx1* and *Vegfr3* that affects the number and morphology of cardiac lymphatic vessels.

We also examined the intestinal lymphatics of the same embryos by LYVE-1 immunostaining. Results revealed that also in this tissue, there was lymphatic vessel hypoplasia in $Tbx1^{Cre/+}$; $Vegfr3^{flox/+}$ embryos, in both the membranous mesentery and in the intestinal wall, compared to controls

TABLE 1 Summary of cardiac lymphatic phenotypes in E18.5 embryos for all genotypes analyzed

	No. of embryos	Number of vessels		Length of vessels		Width of vessels[a]	
		Ventral	Dorsal	Ventral	Dorsal	Ventral	Dorsal
WT	5	100 ± 3.40	100 ± 3.85	100 ± 2.39	100 ± 6.94	100 ± 7.12	100 ± 3.49
$Tbx1^{Cre/+}$	8	107.17 ± 9.39	102.37 ± 13.82	101.60 ± 6.04	106.04 ± 9.73	108.94 ± 23.2	95.02 ± 21.87
$Tbx1^{Cre/+}$; $Vegfr3^{flox/+}$	8	41.57 ± 31.72	56.12 ± 14.81	57.56 ± 21.10	54.17 ± 12.75	285.88 ± 51.1	360.62 ± 101.95
TgVegfr3; $Tbx1^{Cre/+}$; $Vegfr3^{flox/+}$	6	6.12 ± 5.07	70.83 ± 11.63	14 ± 12.39	87.67 ± 7.27	51.28 ± 9.44	148.58 ± 38.07
TgVegfr3; $Tbx1^{Cre/+}$	5	#	103.8 ± 10.68	#	97.70 ± 5.33	#	98.86 ± 3.86
$Tbx1^{Cre/lacZ}$	3	#	#	#	#	#	#
TgVegfr3; $Tbx1^{Cre/lacZ}$	4	#	#	#	#	#	#
WT	5	100 ± 12.14	100 ± 17.70	100 ± 25.37	100 ± 23.69	100 ± 40.93	100 ± 15.45
$Vegfr3^{+/-}$	5	96.58 ± 16.75	92.24 ± 6.75	103.32 ± 15.45	92.17 ± 16.41	250.13 ± 105.2	245.70 ± 73.67

Note: Values expressed as % of WT controls ± standard deviation. #, Vessels absent in most embryos.

[a]Ratio length/area.

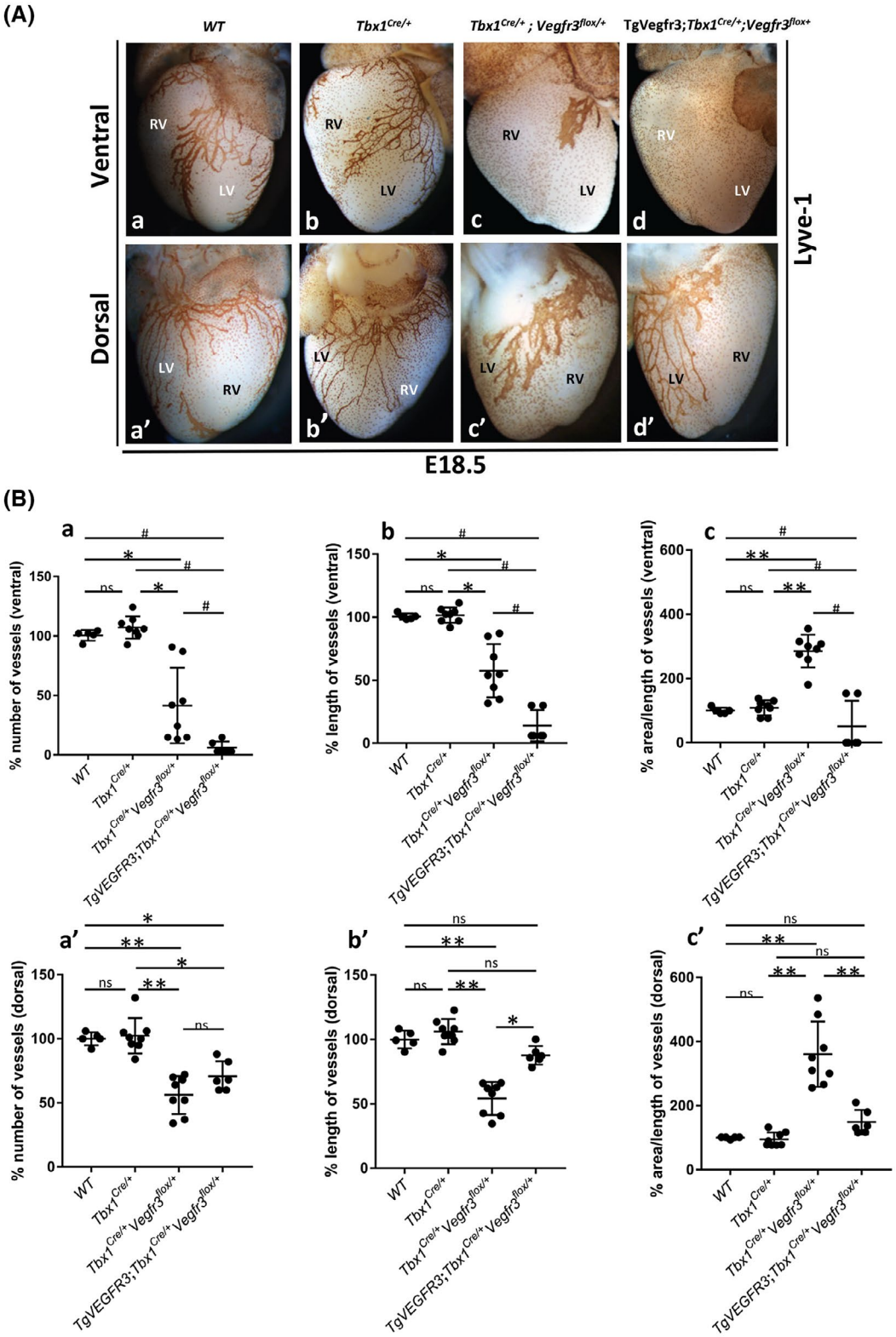

FIGURE 4 *Vegfr3* expression from the TgVegfr3 transgene partially rescues cardiac lymphatic vessel anomalies in *Tbx1-Vegfr3* compound heterozygotes. A, Anti-LYVE1 immunostaining identifies cardiac lymphatic vessels in all genotypes shown (a-d). Hearts of E18.5 *TgVegfr3*; $Tbx1^{Cre/+}$; $Vegfr3^{flox/+}$ embryos (d-d′) reveal partial rescue of lymphatic anomalies observed in $Tbx1^{Cre/+}$; $Vegfr3^{flox/+}$ embryos (c-c′). Quantitative analysis (B) showed rescue of vessel length (b′) and width (c′) but not vessel number (a′) on the dorsal surface of the heart of *TgVegfr3*; $Tbx1^{Cre/+}$; $Vegfr3^{flox/+}$ embryos compared to $Tbx1^{Cre/+}$; $Vegfr3^{flox}$ embryos (c, c′). There was no rescue of ventral lymphatic vessels. LV, left ventricle, RV, right ventricle. $^{*}P < 0.05$, $^{**}P \leq .01$, $^{***}P \leq .001$. Error bars represent standard deviation, #, vessels absent in most *TgVegfr3*; $Tbx1^{Cre/+}$; $Vegfr3^{flox/+}$ embryos (statistical analysis not performed)

(*Tbx1*$^{Cre/+}$, *Vegfr3*$^{+/-}$, WT), although the phenotype was more variable than in the heart (Supporting Figure S2). Thus, we conclude that the genetic interaction between *Tbx1* and *Vegfr3* is not limited to cardiac lymphatic development.

We next sought to gain insights into the cellular basis of the lymphatic vessel phenotype caused by the disruption of the *Tbx1*-Vegfr3 axis. We have previously established that in *Tbx1* mutant mice, the mesenteric lymphatics form but then regress, possibly due to apoptosis.[4] In contrast, in the *Tbx1* homozygous embryos (Supporting Figure S5C-C′), the cardiac lymphatics do not form in the majority of cases, suggesting that a different cellular mechanism is involved. We first tested whether mutation of *Tbx1* and *Vegfr3* affects proliferation of cardiac LECs. To address this, we tested whether proliferation of cardiac LECs is altered by genetic inactivation of *Tbx1* and *Vegfr3* in vivo. For this, we immunostained serial sections of E18.5 hearts of WT, *Tbx1*$^{Cre/+}$, and *Tbx1*$^{Cre/+}$; *Vegfr3*$^{+/-}$ embryos with anti-KI67 and anti-PROX1 antibodies and counted the number of cycling (non G_0) cells (PROX1+; KI67+) compared to the total number of PROX1-labeled cells per heart. Results showed a markedly reduced number of cycling cardiac LECs in the hearts of compound heterozygotes compared to *Tbx1*$^{Cre/+}$ ($P < .01$, n = 1548 cells counted) and WT hearts ($P < .001$, n = 1820 cells counted), but no difference between *Tbx1*$^{Cre/+}$ and WT hearts ($P = .209$, n = 1364 cells counted). Thus, the two mutant alleles have a combined effect on proliferation of PROX1 + cells. We next analyzed the effect of *Tbx1* and *Vegfr3* knockdown (KD) on cell migration in cultured primary human microvascular (HM) LECs by RNA interference. We knocked down expression of *Tbx1* and *Vegfr3* singly and simultaneously in HMLECs and performed a cell migration assay 24 hours after transfection with the siRNAs in a chemotactic gradient, using VEGF-C, a VEGFR3 ligand, as the chemoattractant. Results showed that migration was significantly reduced in all three conditions, with the greatest effect after *Vegfr3* KD (Supporting Figure S3A). In order to elucidate whether these cellular phenotypes might result from altered expression of putative endothelial TBX1 targets (4) (22), we performed quantitative real-time PCR (qRTPCR) on a set of putative targets that includes genes in the Notch pathway[22] in HMLECs. The effect of *TBX1* KD on these genes (Supporting Figure S3B) was similar to that obtained in non-lymphatic EC populations.[22] Specifically, expression of *VEGFR3, DLL4, NRARP,* and *UNC5B* was reduced after *TBX1* KD, while *VEGFR2* expression was slightly increased. Expression of *HEY1* and *NOTCH1* did not change. *VEGFR3* KD reduced the expression of the same genes affected by TBX1 KD, and also of *HEY1* and *NOTCH1,* while it did not affect expression of *TBX1* or *VEGFR2*. Interestingly, there was no evidence of a synergistic effect of simultaneous depletion of *TBX1* and *VEGFR3* on expression of any of the genes analyzed. Genetic deletion of *Vegfr3* in mice has been shown to increase *Vegfr2* expression,[12] as did genetic deletion of *Tbx1*.[22] Moreover, VEGFR2 has been shown to regulate vessel caliber via VEGF signaling.[23] We asked whether increased expression of VEGFR2, albeit modest in cultured HMLECs, could be detected in vivo in cardiac lymphatic vessels. We, therefore, evaluated *Vegfr2* expression in cardiac lymphatics of *Tbx1*$^{Cre/+}$; *Vegfr3*$^{flox/+}$ embryos (E18.5) by co-immunostaining histological sections of the heart with anti-VEGFR2 and anti-LYVE1 antibodies. Results showed no discernible difference in VEGFR2 expression between *Tbx1*$^{Cre/+}$; *Vegfr3*$^{flox/+}$; and *Tbx1*$^{Cre/+}$ (control) hearts (Supporting Figure S3C). Thus, variation of VEGFR2 expression, if present in cardiac lymphatics, is very modest.

3.3 | Vegfr3 overexpression partially rescues cardiac lymphatic defects in *Tbx1-Vegfr3* compound heterozygotes

We next tested whether increasing *Vegfr3* expression in *Tbx1*-expressing tissues, that includes lymphatic ECs, was sufficient to restore normal cardiac lymphatic development in compound heterozygotes. For this, we generated a transgenic mouse, named TgVegfr3, that expresses *Vegfr3* upon Cre-induced recombination. The *Vegfr3*-expressing transgene contains a full-length murine *Vegfr3* cDNA (see Material & Methods and Supporting Figures S4 and S7 for the generation and functional testing of the transgene). We tested whether the TgVegfr3 transgene was able to rescue the cardiac lymphatic vessel anomalies observed in *Tbx1*$^{Cre/+}$; *Vegfr3*$^{flox/+}$ embryos. For this, we crossed *Tbx1*$^{Cre/+}$ mice with TgVegfr3; *Vegfr3*$^{flox/+}$ mice and analyzed cardiac lymphatic vessels in E18.5 embryos with the following genotypes: *Tbx1*$^{Cre/+}$, *Tbx1*$^{Cre/+}$; *Vegfr3*$^{flox/+}$, TgVegfr3; *Tbx1*$^{Cre/+}$; *Vegfr3*$^{flox/+}$ (Figure 4A and Table 1). Results showed that the transgene was able to rescue in part the cardiac lymphatic phenotype observed in compound heterozygotes, described in detail above and shown in Figure 3C, c-c′ and Figure 4A, c-c′. Specifically, on the dorsal surface of the heart of TgVegfr3; *Tbx1*$^{Cre/+}$; *Vegfr3*$^{flox/+}$ embryos (Figure 4A, d′), the lymphatic vessel network was similar in appearance to that of *Tbx1*$^{Cre/+}$ (control) embryos (Figure 4A, b′), being composed of mostly thin, well organized vessels, some of which extended to the apex of the heart. Quantitative analysis confirmed that the abnormal length and width of dorsal lymphatics observed in *Tbx1*$^{Cre/+}$; *Vegfr3*$^{flox/+}$ embryos was fully rescued by the transgene in TgVegfr3; *Tbx1*$^{Cre/+}$; *Vegfr3*$^{flox/+}$ embryos (Figure 4B, d′,c′). In contrast, the reduced number of lymphatic vessels was not rescued (Figure 4B, a′). On the ventral surface of the same hearts, there was no appreciable rescue of the *Tbx1*$^{Cre/+}$; *Vegfr3*$^{flox/+}$ phenotype. In fact, three out of five TgVegfr3; *Tbx1*$^{Cre/+}$; *Vegfr3*$^{flox/+}$ embryos analyzed lacked ventral lymphatics, precluding a statistical

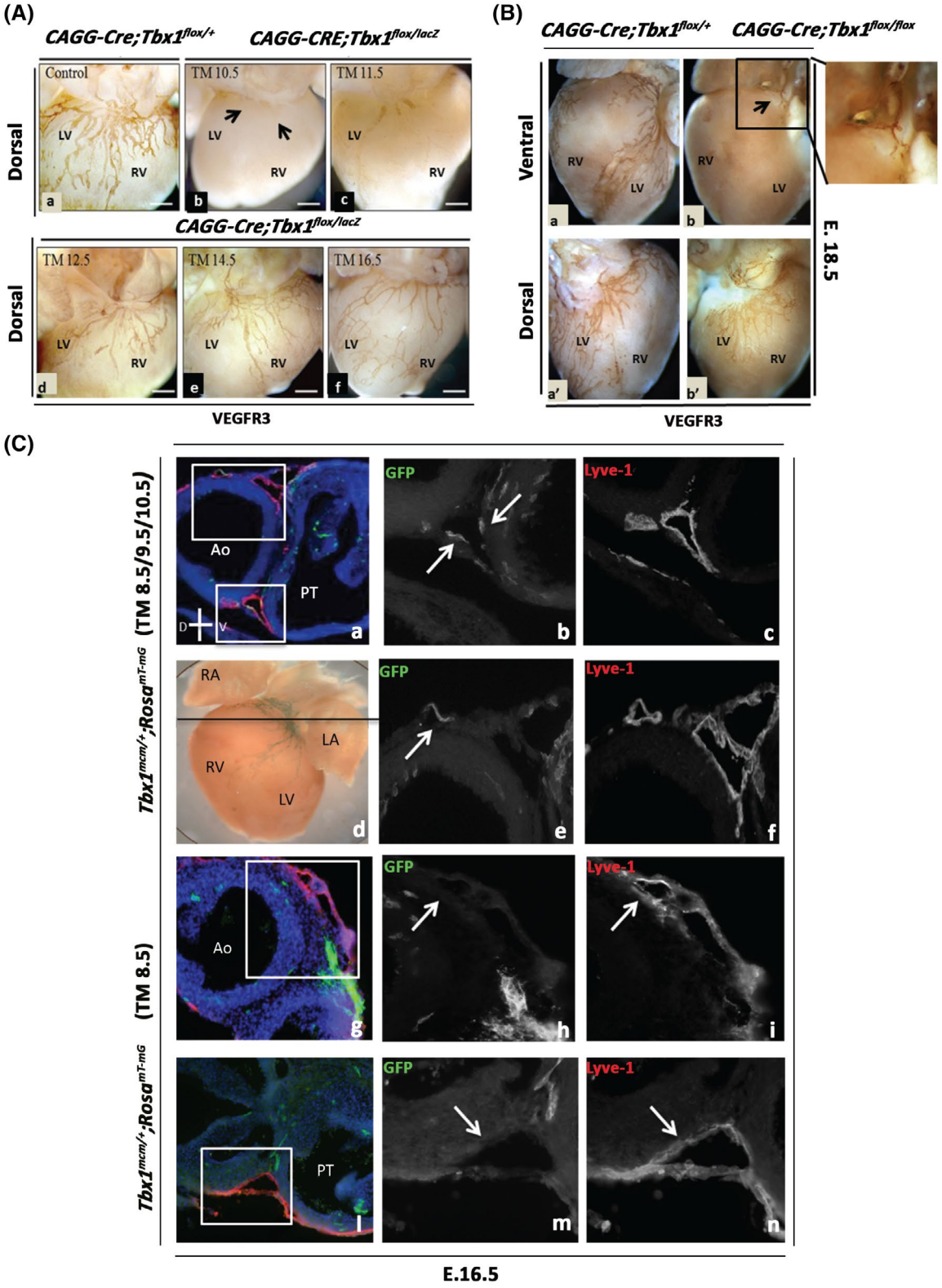

FIGURE 5 Temporal requirement of *Tbx1* for cardiac lymphatic development (A and B). Cardiac lymphatics revealed by VEGFR3 immunostaining of E18.5 hearts following Tamoxifen (TM)-induced inactivation of *Tbx1* between E10.5 and E16.5 (A, b-f) shows that *Tbx1* is required for cardiac lymphangiogenesis before E14.5. B, TM injection at E11.5, revealed a more severe reduction in the number of ventral compared to dorsal cardiac lymphatics in CAGG-CreER; $Tbx1^{flox/flox}$ embryos. *Time-controlled fate mapping of Tbx1-expressing cells* (C). GFP + cells (*Tbx1*-fated) localize to cardiac lymphatics after daily TM induction between E8.5 and E10.5 (a-f) but not after TM induction at E8.5 (g-l). The black line in (d) indicates the position of the transverse section shown in (a). White boxes in (a) are enlarged in (b,c) and (e, f). Scale bar 100 μm. LV, left ventricle, RV, right ventricle, SV, sinus venosus, OFT, outflow tract

analysis. We also tested whether the transgene modified the severe cardiac lymphatic vessel hypoplasia observed in *Tbx1* homozygous embryos,[4] with negative results (Supporting Figure S5, c,c′,d,d′ and Table 1).

Together, these results suggest that establishing the correct number of lymphatic vessels is a VEGFR3-independent TBX1 function. In addition, they suggest that lymphatic vessel hypertrophy in $Tbx1^{Cre/+}$; $Vegfr3^{flox/+}$ embryos is due to reduced dosage of *Vegfr3* in ECs, for which the transgene is able to compensate in *TgVegfr3;* $Tbx1^{Cre/+}$*;* $Vegfr3^{flox/+}$ embryos. Finally, the lack of ventral lymphatics in different genetic mutants, suggests that the *Tbx1-Vegfr3* interaction is required prior to, or at the onset of cardiac lymphangiogenesis.

3.4 | *Tbx1* is activated and required during the early phases of cardiac lymphatic development

We have established that *Tbx1* is expressed in early lymphatic vasculature. In order to gain insights into when *Tbx1* is required for cardiac lymphangiogenesis, we inactivated it in a time-specific manner by crossing CAGG-CreER; $Tbx1^{lacZ/+}$ mice with $Tbx1^{flox/flox}$ mice. We injected pregnant females with a single dose of tamoxifen (TM) at E10.5, E11.5, E12.5, E14.5, and E16.5. We then harvested embryos at E18.5 and analyzed the cardiac lymphatics by VEGFR3 immunostaining (Figure 5A). Results showed that after injection of TM at E10.5 (Figure 5A, b), on the dorsal surface of the heart of CAGG-CreER; $Tbx1^{lacZ/flox}$ embryos, a few lymphatic vessels were present at the sinus venosus (arrows in b) but not on the ventricular myocardium. TM injection at E11.5 and E12.5 (Figure 5A, c,d) resulted in cardiac lymphatic vessel hypoplasia, while after TM injection at E14.5 and E16.5, the lymphatic network was indistinguishable from that of controls (Figure 5A, a,e,f). Given that the peak of recombination occurs 12 hours after TM injection,[15] we conclude that the critical time requirement for *Tbx1* in cardiac lymphangiogenesis is prior to E15, with a strong effect between E10.5 and E11.5. This latter time frame precedes by more than 48 hours the onset of cardiac lymphangiogenesis, suggesting that *Tbx1* plays a critical role in cardiac lymphatic progenitors. However, the extended time requirement for *Tbx1*, that is, until E14.5-E15, which is well after the onset of cardiac lymphangiogenesis, indicates that it is also necessary for the growth of cardiac lymphatics. Interestingly, we noted that after TM injection at E11.5, the ventral cardiac lymphatic network in three out of five CAGG-CreER; $Tbx1^{flox/flox}$ embryos analyzed was severely hypoplastic, while the dorsal network was only mildly affected (Figure 5B). This suggests that *Tbx1* is required earlier in ventral cardiac lymphatic progenitors compared to dorsal progenitors.

In order to gain insights into the timing of *Tbx1* activation in cardiac lymphatic progenitors, we mapped the fate of cells that expressed *Tbx1* in a defined time window. For this, we intercrossed $Tbx1^{mcm/+10}$ and $Rosa^{mT\text{-}mG}$ mice and used TM to induce recombination of the reporter at specific time points. As the $Tbx1^{mcm}$ allele induces low levels of recombination, we first administered three daily i.p. injections of TM to pregnant females at E8.5, E9.5, and E10.5. Embryos were collected at E16.5 and whole hearts (minimum of three per time point) were immunostained with anti-GFP antibody to identify Cre-activated expression of the reporter and anti-LYVE1 antibody to identify lymphatic vessels. Results revealed the presence of GFP + cells in cardiac lymphatics in $Tbx1^{mcm/+}$; $Rosa^{mT\text{-}mG}$ hearts (Figure 5D, a-f). In order to determine the precise timing of this contribution we administered a single injection of TM to pregnant females at E8.5 and E9.5 (one injection per female) and collected and processed embryos at E16.5 as described above. Results showed no contribution of GFP + cells to the cardiac lymphatics of $Tbx1^{mcm/+}$; $Rosa^{mT\text{-}mG}$ hearts exposed to TM at E8.5 (Figure 5D, g-l) or E9.5, although GFP + cells were present in other tissues within the OFT. From this, we deduced that the contribution of GFP + cells to cardiac lymphatics shown in Figure 5D, a-f, was the result of recombination induced by TM at E10.5.

Thus, our data converge on a time window between E10.5 and E11.5 for both the activation of *Tbx1* and its initial requirement. It is then required later, until around E15, for the expansion of the cardiac lymphatic network.

We next determined where *Tbx1* is expressed in putative cardiac lymphatic progenitors in the critical time window. The majority of LECs, including cardiac LECs, derive from *Prox1*-expressing venous progenitors in the anterior cardinal vein (ACV) that transdifferentiate into lymphatic ECs as they delaminate from the ACV between E9.5 and E11 (reviewed in Yang & Oliver 2014).[24] However, recently, a source of putative non-venous cardiac lymphatic progenitors was identified in the pharyngeal mesoderm.[3,20,25] We co-immunostained serial sections of $Tbx1^{Cre/+}$; $Rosa^{mT\text{-}mG}$ embryos at E10.5 and E11.5 with anti-PROX1 and anti-GFP antibodies and analyzed their expression in these two tissues (Figure 6). Interestingly, results showed that *Tbx1*-expressing cells and their progeny (GFP+) do not contribute to PROX1 + LEC progenitors in the ACV (arrowheads in Figure 6A), but GFP+/PROX1 + cells were present in the streams of PROX1 + cells that delaminate from the ACV at this developmental stage (arrows in Figure 6B-D). In the pharyngeal arches (PA) I and II (Figure 6E-H), approximately 50% of PROX1 + cells were GFP+ (arrows in Figure 6E-H). Thus, *Tbx1* is activated in two populations of putative cardiac LEC precursors at the embryonic stage that we determined to be critical by the time-conditional experimental approaches described here.

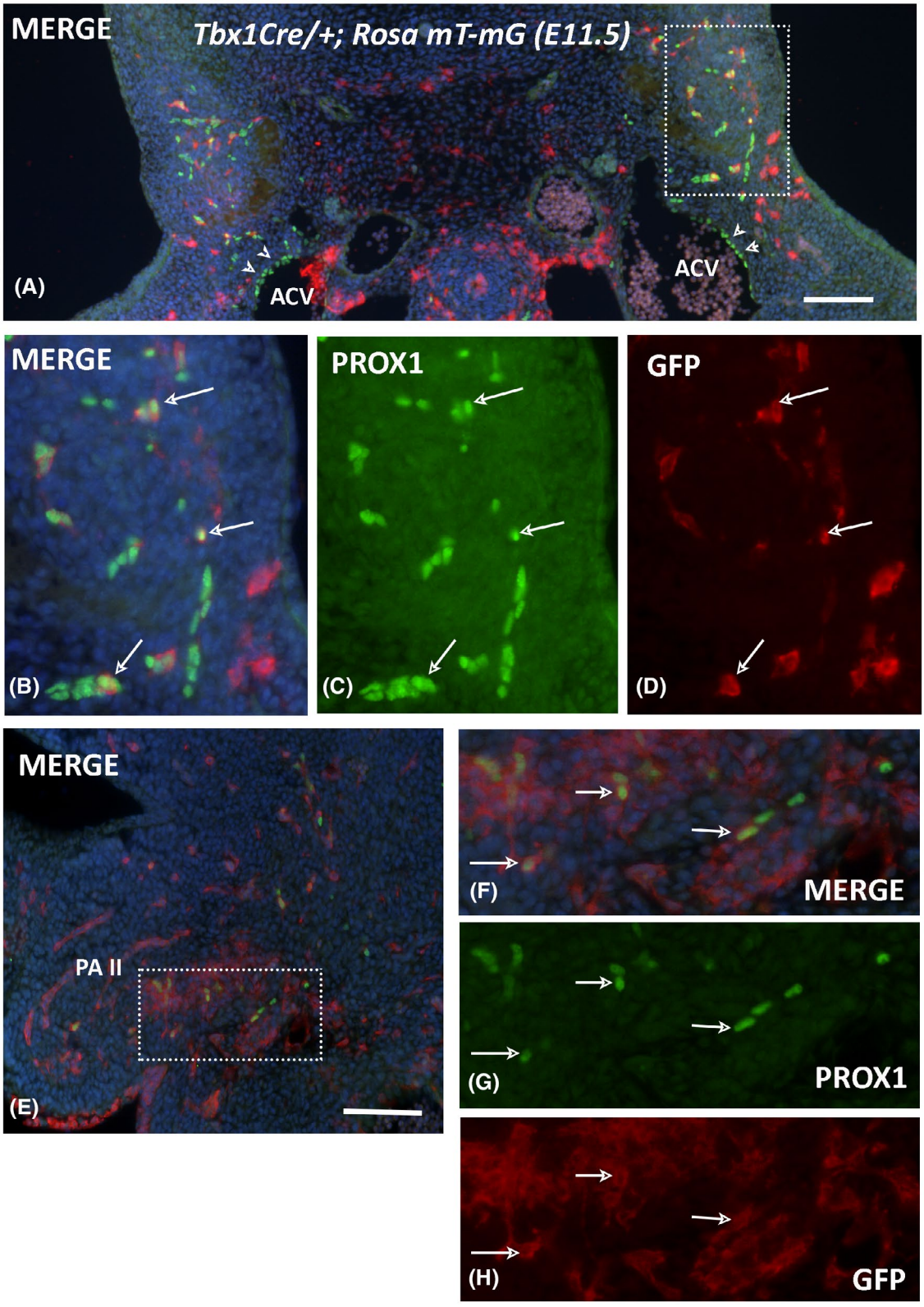

FIGURE 6 TBX1 is activated in putative cardiac LEC progenitors. (A-D) anti-Prox1 and anti-GFP immunostaining of transverse sections of *Tbx1*$^{cre/+}$; *Rosa*$^{mT\text{-}mG}$ embryos at E11.5 reveals TBX1 activation in PROX1-expressing cells (arrows in B-D) in the mesenchyme surrounding the anterior cardinal vein (ACV). PROX1-expressing cells within the ACV (arrowheads in A) do not express TBX1 (GFP-). (E-H) PROX1+; GFP + cells (arrows in F-H) localize to the second pharyngeal arch core mesoderm (GFP+) and surrounding mesenchyme. Scale bars 100 μm. ACV, anterior cardinal vein, PAII, pharyngeal arch

4 | DISCUSSION

In humans, *VEGFR3* heterozygous mutations cause Milroy disease (OMIM 153100), an inherited primary lymphedema that affects the lower limbs. Most of the reported mutations (54/58) are missense mutations within the tyrosine kinase domains 1 and 2 that block the kinase activity of the receptor and interfere with its associated signaling function.[26-28] *Vegfr3*$^{+/-}$ mice were reported to be phenotypically normal,[29] while adult *Chy* mice, which are used as a model of primary lymphedema, have lymphatic hypoplasia and lymphedema. *Chy* mice, carry a heterozygous germline mutation in *Vegfr3* that results in a p.Ile1053Phe substitution, which impairs its kinase activity.[28] The same p.Ile1053Phe substitution has been reported in a patient with Milroy disease.[27] In the present study, we show for the first time that in mice, two functional copies of *Vegfr3* are required for normal cardiac lymphatic development. Specifically, we found that *Vegfr3*$^{+/-}$ embryos had dilated cardiac lymphatics. Lymphatic vessel dilatation has also been reported in *Chy* mutants, affecting the intestinal (subserosal) and cutaneous lymphatic vessels.[28]

Recently, clinical studies have linked *VEGFR3* mutations to congenital heart disease (CHD).[30,31] Intriguingly, in the study by Jin et al dominant *VEGFR3* mutations were found in 2.3% of cases of Tetralogy of Fallot (TOF), which is the most common CHD associated with 22q11.2DS,[32] for which *TBX1* is the major disease gene. Furthermore, Unolt et al reported the presence of primary lymphedema in 4/1600 (0.025%) patients with 22q11.2DS.[33] Prior to this, only a single case report had documented lymphatic abnormalities in a patient diagnosed with DiGeorge syndrome.[34]

The finding of primary lymphedema in 22q11.2DS patients, who have only one functional *TBX1* allele, supports the hypothesis of a *TBX1-VEGFR3* interaction, whereby *TBX1* heterozygosity predisposes to lymphatic anomalies by disrupting the VEGF-C-VEGFR3 signaling pathway. Prior to the publication of the aforementioned studies, we had hypothesized such an interaction on the basis of data obtained in the mouse, which indicated that TBX1 regulates systemic lymphatic vessel development through the VEGF-C-VEGFR3 axis.[4] In the mouse, neo-lymphangiogenesis has been linked to improved recovery after myocardial infarction.[2,5] Therefore, it would be interesting to learn whether post-infarct recovery is compromised in 22q11.2DS patients and to test in the mouse whether *TBX1* has a role in cardiac repair.

In the current study, we found evidence of a strong genetic interaction between *Tbx1* and *Vegfr3* that is critical for cardiac lymphangiogenesis and involves two distinct phenotypes, affecting the number of lymphatic vessels and their morphology. In vivo rescue experiments indicated that these different features of the cardiac lymphatic phenotype are regulated independently by the two genes. Specifically, we found that *Tbx1* primarily regulated the number of lymphatic vessels in a gene dosage-dependent manner that is VEGFR3-independent, based on the following evidence; *Tbx1* homozygotes lack cardiac lymphatics; lymphatic hypoplasia (fewer vessels) in compound *Tbx1-Vegfr3* heterozygotes was not rescued by the TgVegfr3 transgene; *Vegfr3*$^{+/-}$ embryos have the normal number of cardiac lymphatics. In contrast, *Vegfr3* primarily regulated lymphatic vessel morphology; cardiac lymphatic hypertrophy in *Vegfr3*$^{+/-}$ embryos and in compound *Tbx1-Vegfr3* heterozygotes was rescued by TgVegfr3. However, rebalancing *Vegfr3* gene dosage in *Tbx1*-deficient cells was not sufficient to normalize cardiac lymphatic development, suggesting that there are other effectors of TBX1 function in lymphatic ECs, such as Notch signaling. Alternatively, *Tbx1* might have an earlier critical function in cardiac lymphatic EC progenitors, prior to the activation of *Vegfr3*, which is endothelial. We have shown that TBX1 has a role in proliferation and migration of LECs, these effects may explain the defects of extension of the lymphatic network. The effects of TBX1 in cell movement have been reported in multiple cell types, including in the cardiopharyngeal mesoderm.[35-37] These effects could also explain an impairment of LEC progenitor ontogeny, as they are also found in the cardiopharyngeal/pharyngeal mesoderm,[3,25] as we have shown here.

We were intrigued by the different response of ventral vs dorsal cardiac lymphatics to altered *Vegfr3* gene dosage, which was evident in several different genetic mutants. For example, the lymphatic phenotype in compound *Tbx1-Vegfr3* heterozygotes was especially evident on the ventral surface of the heart. Furthermore, the capacity of the TgVegfr3 transgene to rescue the lymphatic phenotype in compound heterozygotes was limited to the dorsal lymphatic network. Finally, overexpression of *Vegfr3* from the TgVegfr3 transgene had a strong effect on ventral but not dorsal cardiac lymphatics. Note that in all three cases, a single copy of *Tbx1* (in *Tbx1*$^{Cre/+}$ embryos) was inactivated, which alone had no effect on cardiac lymphatics. Together, these results suggest that *Tbx1* mutation sensitizes ventral cardiac lymphatics to altered *Vegfr3* gene dosage; note that mild lymphatic hypertrophy in *Vegfr3*$^{+/-}$ mutants affected ventral and dorsal cardiac lymphatics alike. What might be the basis of the differential sensitivity? This study indicates that it might be linked, at least in part, to a different time requirement for *TBX1* in ventral vs dorsal cardiac lymphatic progenitors. The evidence for this comes from the time-controlled *Tbx1* inactivation, which identified a critical time window around E11.5, at which time, inactivation of *Tbx1* led to severe hypoplasia of ventral but not dorsal cardiac lymphatics in CAGG-CreER; *Tbx1*$^{flox/flox}$ embryos. This suggests that *Tbx1* is required earlier in ventral cardiac lymphatic progenitors. The differential time requirement may reflect the different embryological origins of ventral and dorsal cardiac lymphatics that has been

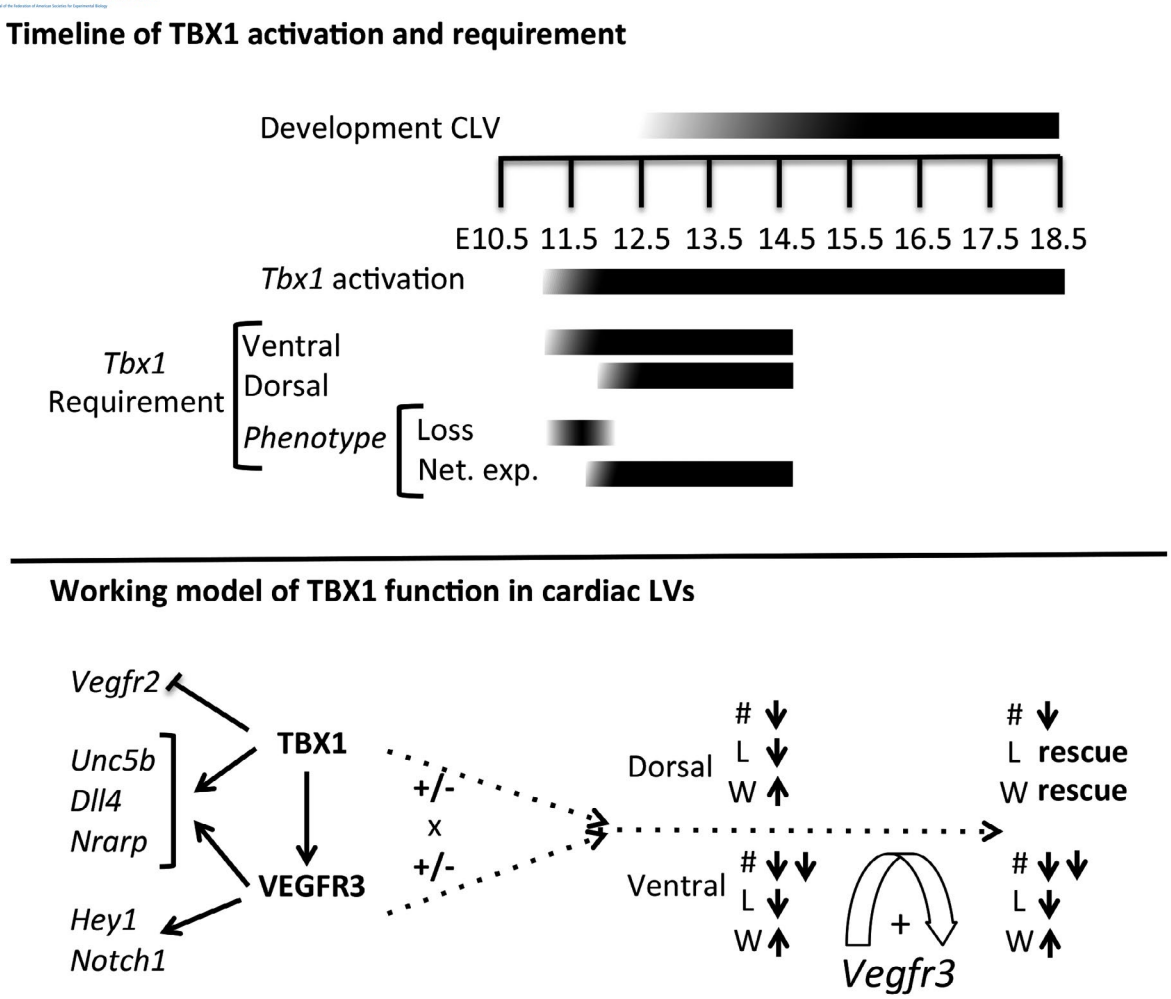

FIGURE 7 Schematic summary of this work. *Top panel*: Timing of TBX1 function. The development of the cardiac lymphatic vessels (CLV) starts with a very few small vessels at around E12.5, but a proper lymphatic vessel network is only visible at around E14.5. The development continues postnatally. *Tbx1* gene activation in lymphatic endothelial cells precursors, as determined by timed cell fate, occurs 24-36 hours before the appearance of vessels. *Tbx1* requirement, determined using timed gene deletion, is earlier in ventral vessels than in dorsal vessels. Phenotypic analyses distinguished two developmental functions, an earlier one that causes complete loss of cardiac lymphatic vessels, and a later one that affects the cardiac lymphatic network extension (Net. exp.). *Bottom panel*: TBX1 regulates and interacts with *Vegfr3* directly, and possibly indirectly, through regulation of Notch signaling components and other genes. Genetic crosses between *Tbx1* and *Vegfr3* heterozygous mutants generated severe lymphatic phenotypes that included a reduced number of vessels (#), vessel length (L) reduction, and width (W) reduction. Additional (transgenic) expression of *Vegfr3* rescued the L and W phenotype, but only in the dorsal side of the heart

reported recently[3] and perhaps, as a consequence, the activation of different transcriptional programs in the two lineages. Other possibilities include, (a) differences in the local molecular environment; several studies have shown that this can profoundly affect VEGFR3 function. For example, VEGFR3 can promote or antagonize angiogenesis through mechanisms that are Notch-dependent and VEGF ligand-independent,[38,39] or there might be differences in expression of VEGF-C or of proteins that activate VEGF-C, (b) increased *Vegfr3* expression in ECs (when the transgene was used) might suppress cardiac lymphangiogenesis. We attempted to address this latter point by generating *TgVegfr3; Tie2*$^{Cre/+}$ embryos, but we did not recover any embryos with the desired genotype at E14.5, indicating that forcing *Vegfr3* expression in all ECs causes lethality prior to the onset of cardiac lymphangiogenesis. Evidently, reducing endogenous *Vegfr3* expression in *TgVegfr3; Tbx1*$^{Cre/+}$*; Vegfr3*$^{flox/+}$ embryos is not sufficient to reduce cardiac lymphatic hypoplasia caused by *Vegfr3* expression from the transgene. This suggests that ectopic *Vegfr3* expression driven by *Tbx1*^{Cre}, for example, in cardiomyocytes of the right ventricle, might be responsible for cardiac lymphatic hypoplasia in these mutants, perhaps by sequestering the ligand, and thus, reducing its availability to lymphatic ECs.

Until recently, the prevailing opinion on the origin of lymphatic vessels was that the vast majority derives from venous EC precursors in the dorsal wall of the anterior cardinal vein, with additional contributions from the intersomitic veins and superficial venous plexus, reviewed in.[24] In recent years, studies of organ-specific lymphangiogenesis

have challenged this view because they have revealed additional, non-venous sources of lymphatic ECs in several different organs, including the skin[40,41] gut[42,43] and heart.[2,3] Most relevant to this study, contributions of non-venous progenitors to cardiac lymphatics have been traced to hemogenic endothelium in the yolk sac[2] and to the pharyngeal mesoderm,[3] part of the cranial mesoderm that includes the secondary heart field.[44] Intriguingly, the embryonic paraxial mesoderm was recently shown to be a critical domain for lymphatic endothelial fate determination globally, as inactivation of *Prox1* in paraxial mesoderm blocked lymphatic development in the mouse.[25] These recent reports are based upon studies that used constitutive Cre drivers, which by definition cannot distinguish between early and current gene activation. In this study, we used a TM-inducible *Tbx1* Cre driver (*Tbx1*^{mcm}), which allowed us to pinpoint the timing of *Tbx1* activation in cardiac lymphatic progenitors. *Tbx1* is expressed in multipotent cardiac progenitors that constitute the anterior portion of the second heart field (aSHF), which gives rise to ECs that populate the aortic arch arteries and the cardiac outflow tract,[10] as well as cardiomyocytes of the inflow and outflow tracts and the right ventricle. We were, therefore, intrigued to know whether these progenitors represent another source of cardiac lymphatic EC precursors. The results of timed *Tbx1* fate mapping experiments indicate that this is unlikely, because they show that *Tbx1* is activated in cardiac LEC progenitors after E10.5, whereas the deployment of aSHF-derived *Tbx1* + cells that contribute to the heart, outflow tract and pharyngeal arch arteries occurs between E8.0 and E9.5.[10,37] At the critical time established in this study, *Tbx1* is expressed (activated) in Prox1-expressing cells in the pharyngeal arches I and II. These putative LEC progenitors might contribute to cardiac lymphatics, as proposed by Maruyama et al,[3] but their location at this stage of development indicates that it is a different population of *Tbx1*-expressing cells to those derived from the aSHF. Thus, our results further delineate the contribution of pharyngeal mesoderm-derived progenitors to cardiac lymphangiogenesis.

In summary, time-controlled experimental approaches strongly point to a dual role for *Tbx1* in cardiac lymphangiogenesis; the first, between E10.5 and E11.5 in cardiac LEC progenitors, and then, later in cardiac lymphatic vessels. We propose a model (Figure 7) where *Tbx1* and *Vegfr3* interact in early forming cardiac lymphatics in order to establish a reciprocal gene dosage equilibrium that determines the correct number and morphology of subepicardial lymphatics and promotes their growth. The nature of this interaction includes, but is probably not only limited to the direct transcriptional regulation of *Vegfr3* by TBX1, but may also include the regulation of additional genes, such as components of the Notch signaling pathway. Other mechanisms may be in place, for example, through cell-to-extracellular matrix signaling pathways, which are altered in *Tbx1* mutants.[35]

ACKNOWLEDGMENTS

We are grateful for the invaluable support provided by the Integrated Microscopy Core and the Animal Facility at the Institute of Genetic and Biophysics "ABT"/CNR, Naples. *Vegfr3*$^{flox/+}$ mice were generously provided by Dr Kari Alitalo. The study was supported by grants from the Fondation Leducq Transatlantic Network of Excellence in Cardiovascular Research, 15CVD01, to EI and AB, from the Jerome Lejeune Foundation, 1685 (to EI), and from the Italian Ministry of Health (RF-2011-02347197) to A.B and #20179J2P9J (to EI and A.B). MGT was supported by a doctoral fellowship from the European School of Molecular Medicine (SEMM).

CONFLICT OF INTEREST

None.

AUTHOR CONTRIBUTIONS

E. Illingworth and A. Baldini conceived the research; S. Martucciello, M.G. Turturo, performed most of the experiments. S. Cioffi and L. Chen assisted with the experiments. M. Bilio provided expert technical support. E. Illingworth and S. Martucciello analyzed the data. E. Illingworth wrote the paper. A. Baldini contributed reagents.

REFERENCES

1. Flaht-Zabost A, Gula G, Ciszek B, et al. Cardiac mouse lymphatics: developmental and anatomical update. *Anat Rec (Hoboken)*. 2014;297:1115-1130.
2. Klotz L, Norman S, Vieira JM, et al. Cardiac lymphatics are heterogeneous in origin and respond to injury. *Nature*. 2015;522:62-67.
3. Maruyama K, Miyagawa-Tomita S, Mizukami K, Matsuzaki F, Kurihara H. Isl1-expressing non-venous cell lineage contributes to cardiac lymphatic vessel development. *Dev Biol*. 2019;452:134-143.
4. Chen L, Mupo A, Huynh T, et al. Tbx1 regulates Vegfr3 and is required for lymphatic vessel development. *J Cell Biol*. 2010;189:417-424.
5. Henri O, Pouehe C, Houssari M, et al. Selective stimulation of cardiac lymphangiogenesis reduces myocardial edema and fibrosis leading to improved cardiac function following myocardial infarction. *Circulation*. 2016;133:1484-1497, discussion 1497.
6. Ishikawa Y, Akishima-Fukasawa Y, Ito K, et al. Lymphangiogenesis in myocardial remodelling after infarction. *Histopathology*. 2007;51:345-353.
7. Lindsay EA, Vitelli F, Su H, et al. Tbx1 haploinsufficieny in the DiGeorge syndrome region causes aortic arch defects in mice. *Nature*. 2001;410:97-101.
8. Xu H, Morishima M, Wylie JN, et al. Tbx1 has a dual role in the morphogenesis of the cardiac outflow tract. *Development*. 2004;131:3217-3227.
9. Huynh T, Chen L, Terrell P, Baldini A. A fate map of Tbx1 expressing cells reveals heterogeneity in the second cardiac field. *Genesis*. 2007;45:470-475.

10. Xu H, Cerrato F, Baldini A. Timed mutation and cell-fate mapping reveal reiterated roles of Tbx1 during embryogenesis, and a crucial function during segmentation of the pharyngeal system via regulation of endoderm expansion. *Development*. 2005;132:4387-4395.
11. Kisanuki YY, Hammer RE, Miyazaki J, Williams SC, Richardson JA, Yanagisawa M. Tie2-Cre transgenic mice: a new model for endothelial cell-lineage analysis in vivo. *Dev Biol*. 2001;230:230-242.
12. Zarkada G, Heinolainen K, Makinen T, Kubota Y, Alitalo K. VEGFR3 does not sustain retinal angiogenesis without VEGFR2. *Proc Natl Acad Sci U S A*. 2015;112:761-766.
13. Soriano P. Generalized lacZ expression with the ROSA26 Cre reporter strain. *Nat. Genet*. 1999;21:70-71.
14. Muzumdar MD, Tasic B, Miyamichi K, Li L, Luo L. A global double-fluorescent Cre reporter mouse. *Genesis*. 2007;45:593-605.
15. Hayashi S, McMahon AP. Efficient recombination in diverse tissues by a tamoxifen-inducible form of Cre: a tool for temporally regulated gene activation/inactivation in the mouse. *Dev Biol*. 2002;244:305-318.
16. Verzi MP, McCulley DJ, De Val S, Dodou E, Black BL. The right ventricle, outflow tract, and ventricular septum comprise a restricted expression domain within the secondary/anterior heart field. *Dev Biol*. 2005;287:134-145.
17. Megason SG, McMahon AP. A mitogen gradient of dorsal midline Wnts organizes growth in the CNS. *Development*. 2002;129:2087-2098.
18. Théveniau-Ruissy M, Pérez-Pomares J-M, Parisot P, Baldini A, Miquerol L, Kelly RG. Coronary stem development in wild-type and Tbx1 null mouse hearts. *Dev Dyn*. 2016;245:445-459.
19. Kaipainen A, Korhonen J, Mustonen T, et al. Expression of the fms-like tyrosine kinase 4 gene becomes restricted to lymphatic endothelium during development. *Proc Natl Acad Sci U S A*. 1995;92:3566-3570.
20. Lioux G, Liu X, Temiño S, et al. A second heart field-derived vasculogenic niche contributes to cardiac lymphatics. *Dev Cell*. 2020;52:350-363.e6.
21. Ehlers ML, Celona B, Black BL. NFATc1 controls skeletal muscle fiber type and is a negative regulator of MyoD activity. *Cell Rep*. 2014;8:1639-1648.
22. Cioffi S, Martucciello S, Fulcoli FG, et al. Tbx1 regulates brain vascularization. *Hum Mol Genet*. 2014;23:78-89.
23. Nakatsu MN, Sainson RCA, Pérez-del-Pulgar S, et al. VEGF(121) and VEGF(165) regulate blood vessel diameter through vascular endothelial growth factor receptor 2 in an in vitro angiogenesis model. *Lab Invest*. 2003;83:1873-1885.
24. Yang Y, Oliver G. Development of the mammalian lymphatic vasculature. *J Clin Invest*. 2014;124:888-897.
25. Stone OA, Stainier DYR. Paraxial mesoderm is the major source of lymphatic endothelium. *Dev Cell*. 2019;50:247-255.e3.
26. Connell FC, Ostergaard P, Carver C, et al. Analysis of the coding regions of VEGFR3 and VEGFC in Milroy disease and other primary lymphoedemas. *Hum Genet*. 2009;124:625-631.
27. Gordon K, Schulte D, Brice G, et al. Mutation in vascular endothelial growth factor-C, a ligand for vascular endothelial growth factor receptor-3, is associated with autosomal dominant milroy-like primary lymphedema. *Circ Res*. 2013;112:956-960.
28. Karkkainen MJ, Saaristo A, Jussila L, et al. A model for gene therapy of human hereditary lymphedema. *Proc Natl Acad Sci U S A*. 2001;98:12677-12682.
29. Dumont DJ, Jussila L, Taipale J, et al. Cardiovascular failure in mouse embryos deficient in VEGF receptor-3. *Science*. 1998;282:946-949.
30. Jin SC, Homsy J, Zaidi S, et al. Contribution of rare inherited and de novo variants in 2,871 congenital heart disease probands. *Nat Genet*. 2017;49:1593-1601.
31. Reuter MS, Jobling R, Chaturvedi RR, et al. Haploinsufficiency of vascular endothelial growth factor related signaling genes is associated with tetralogy of Fallot. *Genet Med*. 2019;21:1001-1007.
32. Unolt M, Versacci P, Anaclerio S, et al. Congenital heart diseases and cardiovascular abnormalities in 22q11.2 deletion syndrome: from well-established knowledge to new frontiers. *Am J Med Genet A*. 2018;176:2087-2098.
33. Unolt M, Barry J, Digilio MC, et al. Primary lymphedema and other lymphatic anomalies are associated with 22q11.2 deletion syndrome. *Eur J Med Genet*. 2018;61:411-415.
34. Mansir T, Lacombe D, Lamireau T, et al. Abdominal lymphatic dysplasia and 22q11 microdeletion. *Genet Couns*. 1999;10:67-70.
35. Alfano D, Altomonte A, Cortes C, Bilio M, Kelly RG, Baldini A. Tbx1 regulates extracellular matrix-cell interactions in the second heart field. *Hum Mol Genet*. 2019;28:2295-2308.
36. Cortes C, Francou A, De Bono C, Kelly RG. Epithelial properties of the second heart field. *Circ Res*. 2018;122:142-154.
37. Rana MS, Théveniau-Ruissy M, De Bono C, et al. Tbx1 coordinates addition of posterior second heart field progenitor cells to the arterial and venous poles of the heart. *Circ Res*. 2014;115:790-799.
38. Benedito R, Rocha SF, Woeste M, et al. Notch-dependent VEGFR3 upregulation allows angiogenesis without VEGF-VEGFR2 signalling. *Nature*. 2012;484:110-114.
39. Tammela T, Zarkada G, Nurmi H, et al. VEGFR-3 controls tip to stalk conversion at vessel fusion sites by reinforcing Notch signalling. *Nat Cell Biol*. 2011;13:1202-1213.
40. Martinez-Corral I, Ulvmar MH, Stanczuk L, et al. Nonvenous origin of dermal lymphatic vasculature. *Circ. Res*. 2015;116:1649-1654.
41. Pichol-Thievend C, Betterman KL, Liu X, et al. A blood capillary plexus-derived population of progenitor cells contributes to genesis of the dermal lymphatic vasculature during embryonic development. *Development*. 2018;145:dev160184.
42. Mahadevan A, Welsh IC, Sivakumar A, et al. The left-right Pitx2 pathway drives organ-specific arterial and lymphatic development in the intestine. *Dev Cell*. 2014;31:690-706.
43. Stanczuk L, Martinez-Corral I, Ulvmar MH, et al. cKit lineage hemogenic endothelium-derived cells contribute to mesenteric lymphatic vessels. *Cell Rep*. 2015;10:1708-1721.
44. Diogo R, Kelly RG, Christiaen L, et al. A new heart for a new head in vertebrate cardiopharyngeal evolution. *Nature*. 2015;520:466-473.

SUPPORTING INFORMATION

Additional supporting information may be found online in the Supporting Information section.

How to cite this article: Martucciello S, Turturo MG, Bilio M, et al. A dual role for *Tbx1* in cardiac lymphangiogenesis through genetic interaction with *Vegfr3*. *The FASEB Journal*. 2020;00:1–18. https://doi.org/10.1096/fj.201902202R